The leading edge is a lipid diffusion barrier

Ina Weisswange[1], Till Bretschneider[2] and Kurt I. Anderson[1,*]

[1]Max Planck Institute of Molecular Cell Biology and Genetics, Pfotenhauerstr. 107, 01307 Dresden, Germany
[2]Max Planck Institute of Biochemistry, Am Klopferspitz 18, 82152 Martinsried, Germany
*Author for correspondence (e-mail: anderson@mpi-cbg.de)

Accepted 10 June 2005
Journal of Cell Science 118, 4375-4380 Published by The Company of Biologists 2005
doi:10.1242/jcs.02551

Summary

Actin polymerization drives many cellular events, including endocytosis, pathogen rocketing, and cell spreading. Force generation and polymerization regulation are intimately linked where an actin meshwork attaches to, and pushes against, an interface. We reasoned that interaction with actin filament plus-ends might stabilize the position of components within the plasma membrane at the leading edge, thereby slowing the diffusion of lipids within the bilayer where filament growth occurs. To test this hypothesis we focally labeled the outer membrane leaflet of migrating keratocytes and compared the initial diffusion of carbocyanine dyes in the dorsal and ventral lamellipodium membranes using sequential TIRF and epi-fluorescent imaging. Global diffusion analysis shows that lateral mobility of lipids in the outer membrane leaflet is blocked at the leading edge during protrusion. Cytochalasin treatment abolished this diffusion barrier, but we found no evidence to support the involvement of membrane microdomains. Our results demonstrate the immobilization of membrane components at the leading edge, and suggest that interaction between actin filaments and the plasma membrane is mediated by densely packed molecular complexes. We propose that actin polymerization traps regulatory proteins at the leading edge in a positive-feedback loop.

Supplementary material available online at
http://jcs.biologists.org/cgi/content/full/118/19/4375/DC1

Key words: Protrusion, Plasma membrane, Actin polymerization

Introduction

How do actin filaments and the plasma membrane interact during force-producing actin polymerization? Current models of actin regulation emphasize the importance of localized activation of the Arp 2/3 complex at a polymerization interface, which has been shown to drive the rocketing motility of intracellular pathogens and beads in vitro and in vivo (Loisel et al., 1999). In vivo Arp 2/3 activators are proposed to function in large molecular complexes comprised of subunits including WASP, WAVE, Sra, Nap, Abi and HSPC300 (Guirland et al., 2004; Stradal et al., 2004), although the exact composition and details of molecular interactions remain unclear. It is also unclear how molecular assemblies remain localized to a dynamic membrane-meshwork interface during the process of filament binding, branching, unbinding and growth, which drives actin-based motility (Carlier et al., 2003). In growth cones recovery of actin polymerization after cytochalasin treatment proceeds from the former leading edge (Forscher and Smith, 1988), which suggests that regulatory factors can remain associated with the folded plasma membrane in the absence of a growing meshwork. Membrane association could be mediated by membrane components such as phosphatidylinositols (Tall et al., 2000), which have been identified as binding partners of N-WASP (Rohatgi et al., 2000) and WAVE2 (Oikawa et al., 2004) and function in chemotaxis (Comer and Parent, 2002). Regulatory assemblies might also be confined within membrane micro-domains (Dietrich et al., 2002), which have been implicated in site-directed actin polymerization during rocketing motility (Pelkmans et al., 2002; Rozelle et al., 2000) and polarized cell motility (Manes et al., 1999).

Fish keratocytes are useful in the study of cell migration due to their unique cellular geometry and persistent migration (Anderson et al., 1996), which is both rapid and non-chemotactic (supplementary material Movie 1). Single particle tracking on keratocytes (Kucik et al., 1990; Sheetz et al., 1989) and fluorescence recovery after photo-bleaching in other cell types (Lee et al., 1990) have shown that no bulk flow of lipids occurs within the plasma membrane during cell migration. Lipids are globally free to diffuse laterally within the membrane, although compartmentalization attributed to 'fences' (Fujiwara et al., 2002; Nakada et al., 2003; Sako and Kusumi, 1995) and 'rafts' (Dietrich et al., 2002; Pralle et al., 2000) has been detected. We reasoned that interaction with actin filament plus-ends might stabilize the position of components within the plasma membrane at the leading edge, thereby slowing the diffusion of lipids within the bilayer where filament growth occurs. To test this hypothesis we developed a method to characterize the global diffusion pattern of lipids within the outer leaflet of the plasma membrane based on focal labeling and the observation of initial diffusion (FLOID) using sequential epi-fluorescence and TIRF microscopy.

Materials and Methods

Cell culture

Fish epidermal keratocytes were cultured from Zebrafish and fixed and stained as described previously (Anderson, 1998). Coverslips were transferred to keratocyte running buffer (KRB) 1-2 hours before membrane labeling or other experimental treatment. All experiments were performed at RT.

Membrane labeling

Dialkylcarbocyanine dyes DiIC12 and DiIC18 (Molecular Probes) were diluted to 1 mg/ml in ethanol and loaded into micro-needles pulled from borosilicate glass capillaries using a Sutter P-30 needle puller. A 50 ml syringe was used to apply holding pressure to the needle, which was mounted in a Leitz Micromanipulator M. The outer surface of the needle tip was coated with dye by squirting some dye out over a coverslip region without cells. The cell body was then touched lightly with the needle to transfer a small amount of dye to the plasma membrane, and a time series of sequential TIRF and epi-illumination was immediately (within 5 seconds) started to observe dye spreading from the point of needle contact. Labeling was performed near the front of the cell body; however, attempts to label the lamellipodium in front of the cell body always ruptured the cell membrane. All cells were selected on the basis of a characteristic canoe shape. Moving cells were further selected for robust motility. Cells immobilized by concanavalin A (CA) were further selected on the basis of active centripetal flow.

Cell treatments

(1) Cells were treated with 0.6 mg/ml CA in KRB for 15 minutes prior to membrane labeling or phalloidin staining.
(2) Cells were treated with CA as described, then transferred into KRB containing 0.6 mg/ml CA + 5 μg/ml cytochalasin B (CB) for 15 minutes prior to membrane labeling or phalloidin staining.
(3) Cells were treated with 3 mM methyl-β-cyclodextrin (CD) for 30 minutes before washing with KRB and membrane labeling. Cholesterol extraction was measured by comparing the ratio of cholesterol to protein for treated and untreated cells using the Amplex Red Cholesterol Assay (Molecular Probes) and the BSA Protein Assay (Pierce). Both assays were performed according to manufacturers instructions.
(4) Cells were incubated for 5 minutes in 2 μg/ml of Alexa-488-conjugated cholera toxin (Molecular Probes) and then washed with KRB prior to epi-fluorescent imaging.

Microscopy

Sequential TIRF and epi-fluorescent imaging was performed using an Olympus IX-71 microscope equipped with a 60×, 1.45 NA objective and 2× intermediate magnification. Evanescent wave and epi-illumination were accomplished using a TILL-Photonics condensor. 488 nm laser light was delivered via fiber coupling from an Innova 70c laser using an Opto Electronics AOTF for line selection, shuttering and intensity control. Epi-illumination was delivered via fiber coupling from an Olympus 100W HG lamp with a Uni-blitz shutter. During sequential acquisition, the TIRF image preceded the epi-illumination image by 750 milliseconds. The fluorescence filter cube of the microscope contained a 488/10 excitation filter, 500 dichroic, and 505 LP emission filter. Images were acquired using a MicroMax 512BFT CCD camera. All components were controlled using MetaMorph software. Owing to the thinness of the lamellipodium, fluorescence intensity from the dorsal and ventral cell surfaces contributed equally to the epi-fluorescent images. By contrast, evanescent field illumination restricted fluorescence excitation to a thin region near the coverslip surface (typically ~150 nm), producing images of the bottom of the cell only (Fig. 1). This optical distinction was confirmed by imaging fluorescent beads on cells; only beads lying directly on the glass coverslip, but not those lying on the 200 nm thick lamellipodium surface, were imaged by the evanescent field (supplementary material Fig. S1).

Estimation of diffusion constants

Fluorescence along five parallel, 1 pixel (0.11 μm)-wide section lines of the leading lamella perpendicular to the leading edge were sampled and averaged. The frame to frame interval for most cases was 1.9 seconds. The curves obtained were fitted to an exponential function, $f(x)=b + a*\exp(-k*x)$, using a Levenberg-Marquardt algorithm doing nonlinear regression. Pairs of subsequent fits for a particular cell were chosen that resulted in the minimum total sum of squares of residuals for two subsequent curves. This applied in most cases to the very early onset of diffusion. Diffusion constants were obtained by using centered differences for computing intensity gradients of the fitted curves.

Results

Lipid diffusion is blocked around the leading edge

The leading edge is a dynamic interface where force is applied by the actin meshwork to the plasma membrane. To see if membrane lipids could diffuse from cell top to bottom around the leading edge during protrusion, locomoting keratocytes were labeled with DiIC12 on the cell body, followed by immediate sequential TIRF and epi-fluorescence time-lapse imaging (Fig. 1). Note that epi-fluorescent illumination excites fluorophores in both the dorsal and ventral membranes of the lamellipodium, whereas TIRF illumination excites dye only in the ventral lamellipodium membrane (supplementary material Fig. S1). Epi-fluorescent images show that DiIC12 spread rapidly from the point of labeling to evenly cover the entire cell surface within 30 seconds (supplementary material Movie 2). TIRF images showed that dye continuously spread from the dorsal to ventral membrane around the back of the cell body. Analysis of merged TIRF and epi images from DiIC12-labeled cells revealed that dye always reached the leading edge first via the dorsal membrane (epi), but revealed two distinct profiles of dye spreading across the ventral cell surface (TIRF). Cells were classified according to the TIRF intensity profile after dye first appeared at the leading edge on the ventral surface (Fig. 2). The single peak profile (Fig. 2A,C) indicates that dye spread to the ventral surface via the rear of the cell body only. For this case, careful comparison of TIRF and epi-fluorescence intensity profiles at the leading edge (Fig. 2F-I) revealed that

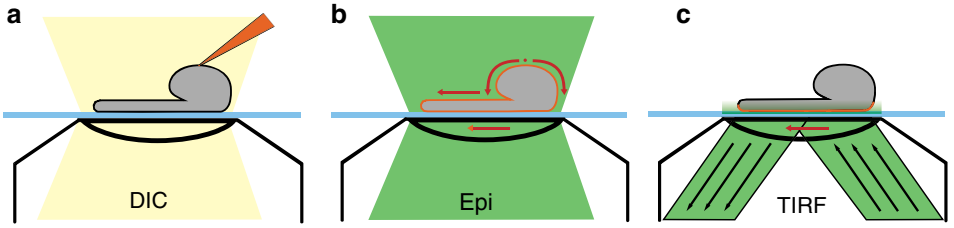

Fig. 1. Schematic diagram of focal labeling and observation of initial diffusion (FLOID). (a) The cell body is lightly touched by a micro-needle containing carbocyanine dye. (b) Epi-illumination shows dye spreading in both dorsal and ventral cell membranes. The shortest diffusion path from the labeling point to the leading edge is via the dorsal membrane. (C) TIRF illumination shows only the ventral cell membrane.

dye began to accumulate on the dorsal surface without spreading to the ventral surface, i.e. diffusion from the dorsal to ventral cell surface was blocked at the leading edge (Fig. 2I, arrow). Continuous accumulation of dye on the dorsal surface was observed for up to 7 seconds prior to dye reaching the leading edge via the ventral surface (supplementary material Movie 3). By contrast, the double peak profile (Fig. 2B,D) shows that diffusion from the dorsal to ventral surface has occurred at both the front and rear of the cell. Single- and double-peak intensity profiles were never observed to interconvert. The single peak profile was observed in 86% of cells (n=138, Fig. 2E). Retracting regions of the leading edge also demonstrated the double peak profile. From this we conclude that a continuously protruding leading edge is a barrier to the lateral diffusion of DiIC12.

The barrier depends on actin polymerization

To test the dependence of diffusion inhibition on free actin filament plus-ends, cells were treated with the drug cytochalasin B (CB), which tightly binds plus-ends to block interaction with other proteins. This treatment disrupts filament treadmilling, resulting in rapid depolymerization of F-actin and dramatic morphological changes in motile cells including loss of lamellipodium (Anderson et al., 1996). To preserve the cell morphology necessary for membrane diffusion analysis, keratocytes were first immobilized using the lectin concanavalin A (CA), an agent commonly used to increase cell adhesion and spreading (Rogers et al., 2003). CA treatment stopped cell locomotion and induced centripetal flow in the lamellipodium (supplementary material Movie 4). Centripetal flow indicates that actin polymerization was still active, although some disorganization of the lamellipodium actin meshwork was apparent (Fig. 3A,C). FLOID analysis revealed that the leading-edge lipid diffusion barrier was present in 51% of CA-immobilised cells undergoing centripetal flow (Fig. 4A). Analysis of dye spreading on the ventral surface of CA-immobilized cells resulted in a diffusion constant of $3.9\pm1.8\times10^{-8}$ cm^2/s (errors represent the standard deviation of the mean, n=9 cells), in agreement with the value of $1.3\pm0.8\times10^{-8}$ cm^2/s (n=10) determined by FRAP analysis of these cells. CA-immobilised cells treated with CB remained well spread, but lost the actin meshwork within the lamellipodium (Fig. 3D) and stopped centripetal flow. The

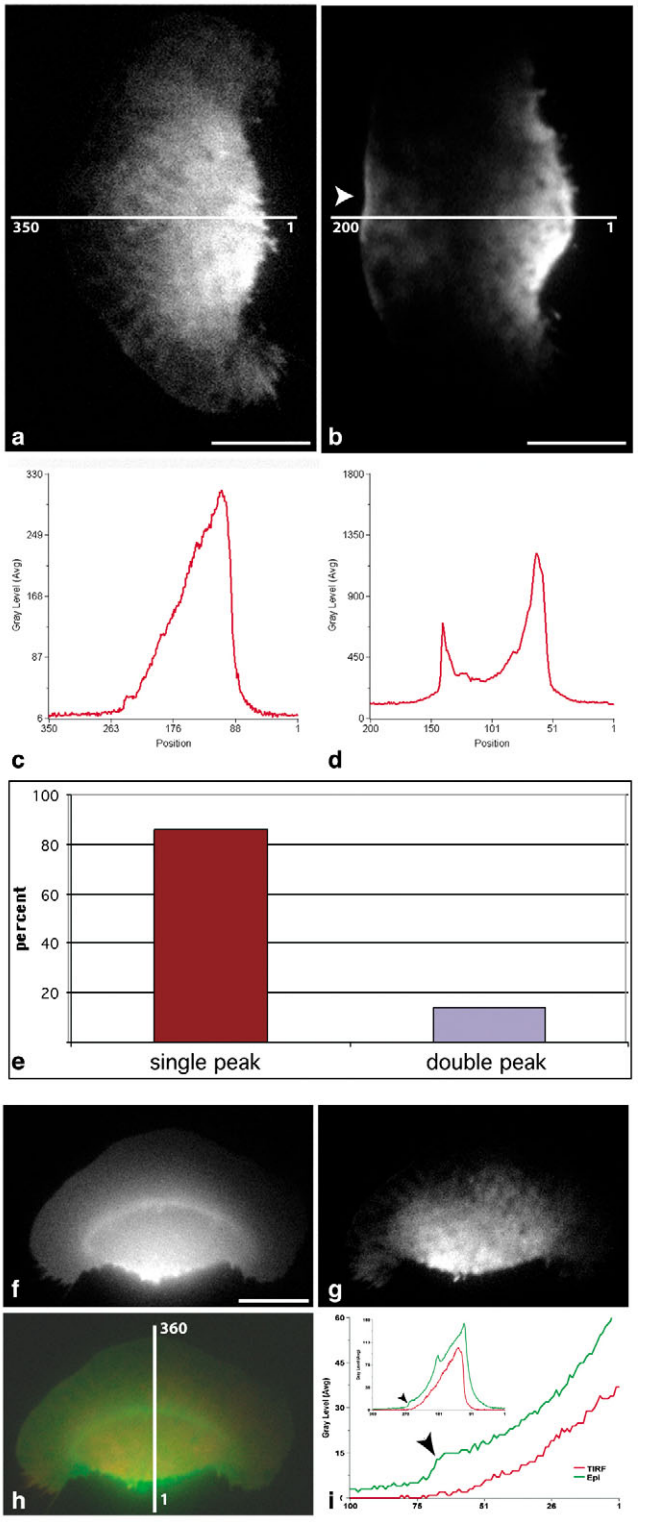

Fig. 2. FLOID analysis of migrating keratocytes. TIRF images (a and b) show the location in which dye has spread from the dorsal to ventral cell surface; either at the back of the cell only (single peak, a and c) or both at the front and back (double peak, b and d). Undulations in the ventral cell surface have been shown previously using interference reflection microscopy (Anderson and Cross, 2000), and lead to variations in dye excitation according to the distance of the cell surface from the coverslip. White bars (a and b) show the position used for fluorescence intensity scans in c and d, respectively. Arrowhead (b) indicates a region of reduced protrusion at the leading edge, where dye has spread from the dorsal to ventral cell membrane. Comparison of sequentially acquired epi-fluorescent (f) and TIRF (g) images from the same cell, and the overlay (h). Note that TIRF proceeds epi-fluorescent illumination by 750 milliseconds. The white bar (h) shows the position used for fluorescence intensity scans in i. (i) The epi-fluorescence intensity scan (green line) indicates that dye has spread from the back of the cell toward the front, and begun to accumulate at the leading edge (arrowhead). The TIRF intensity scan (red line) also shows that dye has spread from the back of the cell toward the front, but not yet reached the leading edge. Note that accumulated dye in the dorsal membrane has not spread around the leading edge to the ventral surface. Inset shows profile for the whole cell. 86% of cells analyzed (n=138) were found to show the single-peak intensity profile (e). Bars, 10 μm.

diffusion barrier was abolished in 96% of CA/CB-treated cells (Fig. 4A; see also supplementary material Movie 5). The same result was achieved using cytochalasin D instead of cytochalasin B (I. König, personal communication). After CB washout, actin polymerization proceeded from the former leading edge, similarly to recovery from CB treatment in *Aplysia* growth cone (Forscher and Smith, 1988). This indicates that neither polymerization governing factors, which remained associated with the leading edge during drug treatment, nor membrane curvature alone were sufficient to inhibit membrane diffusion in the absence of a growing meshwork. From these results we conclude that inhibition of lateral membrane diffusion at the leading edge depends on free actin filament plus ends.

The barrier does not depend on lipid microdomains

The segregation of lipids and/or microdomains has been implicated in polarized cell migration (Gomez-Mouton et al., 2004; Guirland et al., 2004) as well as site-directed actin polymerization (Pelkmans et al., 2002). One possible explanation for the lipid diffusion barrier at the leading edge would be if the leading edge were one continuous lipid domain that excluded DiIC12. We took three approaches to test the involvement of lipid micro-domains in the leading-edge lipid diffusion barrier. First, we compared the ability of carbocyanine dyes that had shorter (DiIC12) or longer (DiIC18) acyl chains to diffuse around the leading edge of locomoting keratocytes. Based on differences in acyl chain length, these dyes might show different mobilities through lipid microdomains concentrated at the leading edge. However diffusion of the two dyes was equally inhibited (Fig. 4B). Furthermore, neither dye was enriched at the leading edge. A hallmark of liquid-ordered domains is their sensitive dependence on membrane cholesterol (Kahya et al., 2004). In a second approach, we therefore used methyl-β-cyclo-dextran treatment to extract 35% of plasma membrane cholesterol from keratocytes prior to FLOID. Similar treatment has been shown to disrupt membrane domain organization in murine fibroblasts (Dietrich et al., 2002), polarized T cells (Gomez-Mouton et al., 2001), and *Xenopus* neurons (Guirland et al., 2004). Keratocyte morphology and motility were unchanged by this treatment, and the number of cells showing a diffusion barrier was marginally reduced from 86% to 75% (Fig. 4B). Cholesterol extraction also reduced the intensity of phalloidin staining by 25% (n=40) compared with that in untreated cells (Fig. 3B), which suggests a link between the diffusion barrier reduction and actin filament density. Finally, cells were treated with fluorescently conjugated cholera toxin, which binds

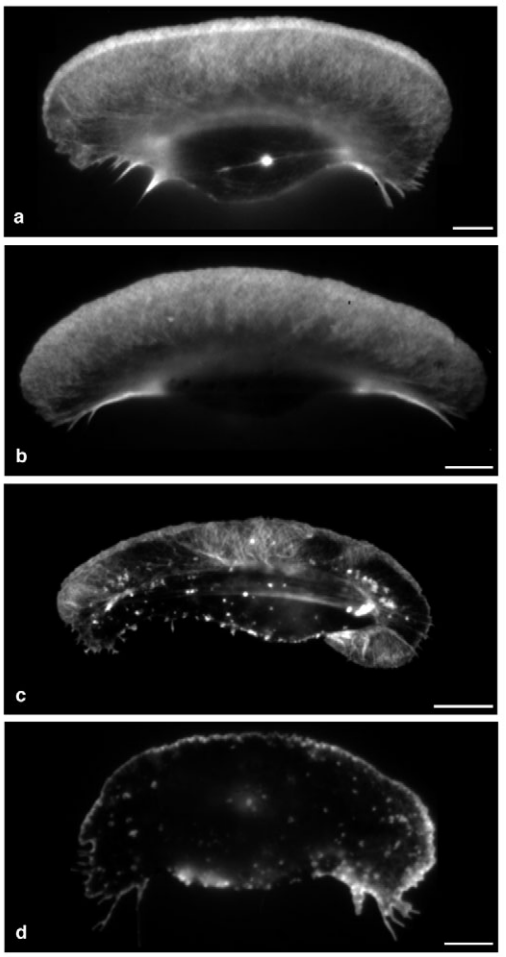

Fig. 3. Keratocytes stained with Alexa-488 phalloidin to reveal F-actin distribution after (a) no treatment, (b) extraction of membrane cholesterol with CD, (c) treatment with CA to stop motility, and (d) CA/CB treatment to depolymerise the actin meshwork. The fluorescence intensity of phalloidin stain was reduced by 25% in CD-treated cells compared with controls. Fluorescence intensities cannot be compared directly in these images because they are displayed on different contrast scales. Bars, 5 μm.

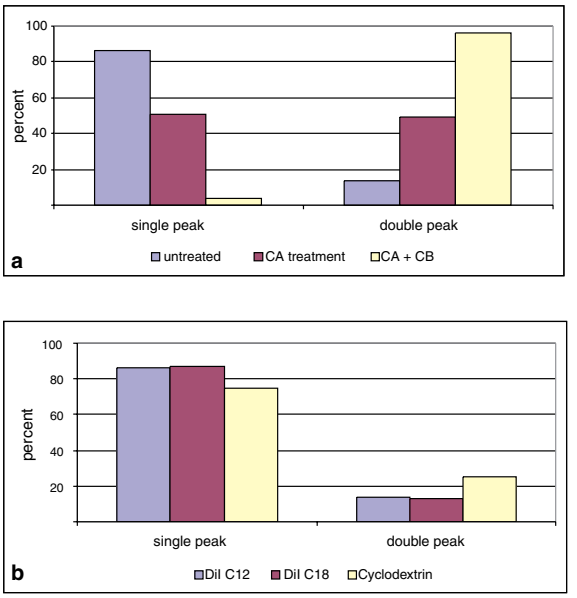

Fig. 4. Number of cells showing blocked dye diffusion at the leading edge (single peak intensity scan) under different labelling conditions. (a) CA treatment reduced the fraction of single peak cells from 86% (n=138) to 51% (n=45). CA/CB treatment further reduced this value to 4% (n=49). (b) The diffusion of carbocyanine dyes that have different acyl chain lengths was equally inhibited during protrusion at the leading edge. Extraction of 35% of cholesterol by CD treatment marginally reduced the fraction of single peak cells from 86% to 75% (n=36).

specifically to the liquid-ordered phase marker GM1. Cells labeled with cholera toxin continued to move normally for up to 60 minutes. Labeling was homogenous with no enrichment at either the front or rear of the cell (supplementary material Movie 6). From this we conclude that inhibition of carbocyanine diffusion at the leading edge does not depend on lipid micro-domains.

Discussion

We have developed a new appproach to the analysis of membrane dynamics based on Focal Labeling and Observation of Initial Diffusion (FLOID) using sequential TIRF and epi-fluorescent imaging. Quantitative analysis of FLOID and FRAP data resulted in similar values for the diffusion constant of DiIC12 in the keratocyte plasma membrane. Compared to FRAP, however, FLOID directly visualizes global patterns in diffusion, especially diffusion inhibition. The type of diffusion barrier we sought to detect using FLOID would not be detectable using FRAP performed in a laser scanning microscope owing to the symmetry of bleaching in the dorsal and ventral membranes of the 200-nm-thick lamellipodium.

The leading edge is a unique location, where regulation of actin polymerization, and force generation by actin filaments on the plasma membrane occur. The demonstration in rocketing motility assays that beads and bacteria are attached to their actin tails, while being pushed by them, has placed important limits on the mechanism of force generation. Two current models of force generation by actin polymerization, the tethered filament (Mogilner and Oster, 2003) and elastic shear stress (Gerbal et al., 2000) models, both distinguish between a small fraction of filaments that bind the membrane and restrain progress of the leading edge, and the majority of filaments which push on the membrane but remain free to bend away and add new monomers. However, direct interaction between an actin meshwork and the plasma membrane fold of the leading edge has not previously been demonstrated. We hypothesized that contact between actin filaments and the plasma membrane might inhibit lipid diffusion at the leading edge, and have detected such a barrier through the analysis of global diffusion patterns using FLOID.

During normal protrusion, diffusion around the leading edge was blocked in 86% of cells. The diffusion barrier was reduced to 51% of CA immobilized cells undergoing centripetal flow, where the actin meshwork of the lamellipodium was disorganized compared with that in controls. Likewise, a small reduction in presence of the diffusion barrier was associated with 25% reduction in actin filament density in CD-treated cells. Finally, the diffusion barrier was reduced to 4% of cytochalasin-treated cells, which had no filament meshwork in the lamellipodium. Taken together these data demonstrate a link between the actin filament meshwork and diffusion barrier at the leading edge. To understand the basis of the double-peak profile, further studies are required to correlate the rate of diffusion around the leading edge with the local density of actin filaments and/or polymerization regulators such as WASP family proteins.

By contrast, several lines of investigation found no support for the dependence of the diffusion barrier on lipid microdomains. Lipid dyes that have either short or long acyl-chains behaved identically with respect to diffusion inhibition. Neither these dyes nor the specific raft marker GM1 showed any sign of differential localization in the plasma membrane, which would indicate the zonal distribution of lipids or domains. And finally, a substantial extraction of membrane cholesterol reduced the diffusion barrier by an insubstantial amount. The non-involvement of lipid microdomains is consistent with previous suggestions that microdomains have no role in the basic mechanism of protrusion but function instead in the directed response to external cues (Manes et al., 1999).

The distribution of actin filaments at the leading edge is too sparse (1 filament per 1570 nm^2) (Abraham et al., 1999; Small et al., 1995) to block the passage of sub-nanometer radius lipid molecules. Therefore the diffusion barrier must be mediated by protein intermediaries organized into a dense array, sufficiently tight-knit to prohibit the crossing of lipid molecules. Inhibition of dye diffusion in the outer membrane leaflet could be mediated by inter-bilayer coupling between lipid acyl-chains in the inner and outer membrane leaflets (Dietrich et al., 2001), or the action of trans-membane proteins (see below). It is not unreasonable to suppose that the force of actin filaments pushing on the plasma membrane plays a role in generating the diffusion barrier, as opposed to the presence of actin filaments merely stabilizing the position of membrane components. Protein-based lipid diffusion barriers, which depend on the underlying actin cytoskeleton, have been demonstrated in rat hippocampal neuron (Nakada et al., 2003) and fibroblast (Fujiwara et al., 2002) plasma membrane. Similar ‘fence’ mechanisms may be in operation here; however, the unique structural and kinetic properties of the leading edge impose serious constraints. First, the leading edge is a dynamic interface, which constantly changes position relative to the stationary meshwork of the lamellipodium. Second, actin filaments terminate at angles of approximately 45 degrees to the leading edge (Small et al., 1995), but there are no filaments running parallel to the edge that could act as a scaffolding for transmembrane-receptor-mediated inhibition of diffusion according to membrane fence models (Fujiwara et al., 2002; Nakada et al., 2003).

Finally, we speculate that the leading-edge lipid diffusion barrier could function in the regulation of actin polymerization by trapping regulatory factors, such as the WAVE complex or their membrane docking sites, at the leading edge. In this way, only the signal to initiate actin polymerization would require active localization to the plasma membrane. Once the necessary critical mass of components were recruited, polymerization would continue due to trapped activators. Additional work is required to identify the molecular complexes that mediate inhibition of lipid diffusion at the leading edge by connecting actin filaments to the plasma membrane.

We thank the Simons and Thiele labs for help with the cholesterol depletion experiments, and Kai Simons, Christian Dietrich and Nicoletta Kahya for encouraging discussion and critical reading of the manuscript.

References

Abraham, V. C., Krishnamurthi, V., Taylor, D. L. and Lanni, F. (1999). The actin-based nanomachine at the leading edge of migrating cells. *Biophys. J.* **77**, 1721-1732.

Anderson, K. and Small, J. V. (1998). Preparation and fixation of fish keratocytes. In *Cell Biology: A Laboratory Handbook*, Vol. 2 (ed. J. E. Celis), pp. 372-376. San Diego: Academic Press.

Anderson, K. I. and Cross, R. (2000). Contact dynamics during keratocyte motility. *Curr. Biol.* **10**, 253-260.

Anderson, K. I., Wang, Y. L. and Small, J. V. (1996). Coordination of protrusion and translocation of the keratocyte involves rolling of the cell body. *J. Cell Biol.* **134**, 1209-1218.

Carlier, M. F., Le Clainche, C., Wiesner, S. and Pantaloni, D. (2003). Actin-based motility: from molecules to movement. *BioEssays* **25**, 336-345.

Comer, F. I. and Parent, C. A. (2002). PI 3-kinases and PTEN: how opposites chemoattract. *Cell* **109**, 541-544.

Dietrich, C., Bagatolli, L. A., Volovyk, Z. N., Thompson, N. L., Levi, M., Jacobson, K. and Gratton, E. (2001). Lipid rafts reconstituted in model membranes. *Biophys. J.* **80**, 1417-1428.

Dietrich, C., Yang, B., Fujiwara, T., Kusumi, A. and Jacobson, K. (2002). Relationship of lipid rafts to transient confinement zones detected by single particle tracking. *Biophys. J.* **82**, 274-284.

Forscher, P. and Smith, S. J. (1988). Actions of cytochalasins on the organization of actin filaments and microtubules in a neuronal growth cone. *J. Cell Biol.* **107**, 1505-1516.

Fujiwara, T., Ritchie, K., Murakoshi, H., Jacobson, K. and Kusumi, A. (2002). Phospholipids undergo hop diffusion in compartmentalized cell membrane. *J. Cell Biol.* **157**, 1071-1081.

Gerbal, F., Chaikin, P., Rabin, Y. and Prost, J. (2000). An elastic analysis of Listeria monocytogenes propulsion. *Biophys. J.* **79**, 2259-2275.

Gomez-Mouton, C., Abad, J. L., Mira, E., Lacalle, R. A., Gallardo, E., Jimenez-Baranda, S., Illa, I., Bernad, A., Manes, S. and Martinez, A. C. (2001). Segregation of leading-edge and uropod components into specific lipid rafts during T cell polarization. *Proc. Natl. Acad. Sci. USA* **98**, 9642-9647.

Gomez-Mouton, C., Lacalle, R. A., Mira, E., Jimenez-Baranda, S., Barber, D. F., Carrera, A. C., Martinez, A. C. and Manes, S. (2004). Dynamic redistribution of raft domains as an organizing platform for signaling during cell chemotaxis. *J. Cell Biol.* **164**, 759-768.

Guirland, C., Suzuki, S., Kojima, M., Lu, B. and Zheng, J. Q. (2004). Lipid rafts mediate chemotropic guidance of nerve growth cones. *Neuron* **42**, 51-62.

Kahya, N., Scherfeld, D., Bacia, K. and Schwille, P. (2004). Lipid domain formation and dynamics in giant unilamellar vesicles explored by fluorescence correlation spectroscopy. *J. Struct. Biol.* **147**, 77-89.

Kucik, D. F., Elson, E. L. and Sheetz, M. P. (1990). Cell migration does not produce membrane flow. *J. Cell Biol.* **111**, 1617-1622.

Lee, J., Gustafsson, M., Magnusson, K. E. and Jacobson, K. (1990). The direction of membrane lipid flow in locomoting polymorphonuclear leukocytes. *Science* **247**, 1229-1233.

Loisel, T. P., Boujemaa, R., Pantaloni, D. and Carlier, M. F. (1999). Reconstitution of actin-based motility of Listeria and Shigella using pure proteins. *Nature* **401**, 613-616.

Manes, S., Mira, E., Gomez-Mouton, C., Lacalle, R. A., Keller, P., Labrador, J. P. and Martinez, A. C. (1999). Membrane raft microdomains mediate front-rear polarity in migrating cells. *EMBO J.* **18**, 6211-6220.

Mogilner, A. and Oster, G. (2003). Force generation by actin polymerization II: the elastic ratchet and tethered filaments. *Biophys. J.* **84**, 1591-1605.

Nakada, C., Ritchie, K., Oba, Y., Nakamura, M., Hotta, Y., Iino, R., Kasai, R. S., Yamaguchi, K., Fujiwara, T. and Kusumi, A. (2003). Accumulation of anchored proteins forms membrane diffusion barriers during neuronal polarization. *Nat. Cell. Biol.* **5**, 626-632.

Oikawa, T., Yamaguchi, H., Itoh, T., Kato, M., Ijuin, T., Yamazaki, D., Suetsugu, S. and Takenawa, T. (2004). PtdIns(3,4,5)P3 binding is necessary for WAVE2-induced formation of lamellipodia. *Nat. Cell Biol.* **6**, 420-426.

Pelkmans, L., Puntener, D. and Helenius, A. (2002). Local actin polymerization and dynamin recruitment in SV40-induced internalization of caveolae. *Science* **296**, 535-539.

Pralle, A., Keller, P., Florin, E. L., Simons, K. and Horber, J. K. (2000). Sphingolipid-cholesterol rafts diffuse as small entities in the plasma membrane of mammalian cells. *J. Cell Biol.* **148**, 997-1008.

Rogers, S. L., Wiedemann, U., Stuurman, N. and Vale, R. D. (2003). Molecular requirements for actin-based lamella formation in Drosophila S2 cells. *J. Cell Biol.* **162**, 1079-1088.

Rohatgi, R., Ho, H. Y. and Kirschner, M. W. (2000). Mechanism of N-WASP activation by CDC42 and phosphatidylinositol **4**, 5-bisphosphate. *J. Cell Biol.* **150**, 1299-1310.

Rozelle, A. L., Machesky, L. M., Yamamoto, M., Driessens, M. H., Insall, R. H., Roth, M. G., Luby-Phelps, K., Marriott, G., Hall, A. and Yin, H. L. (2000). Phosphatidylinositol 4,5-bisphosphate induces actin-based movement of raft-enriched vesicles through WASP-Arp2/3. *Curr. Biol.* **10**, 311-320.

Sako, Y. and Kusumi, A. (1995). Barriers for lateral diffusion of transferrin receptor in the plasma membrane as characterized by receptor dragging by laser tweezers: fence versus tether. *J. Cell Biol.* **129**, 1559-1574.

Sheetz, M. P., Turney, S., Qian, H. and Elson, E. L. (1989). Nanometre-level analysis demonstrates that lipid flow does not drive membrane glycoprotein movements. *Nature* **340**, 284-288.

Small, J. V., Herzog, M. and Anderson, K. (1995). Actin filament organization in the fish keratocyte lamellipodium. *J. Cell Biol.* **129**, 1275-1286.

Stradal, T. E., Rottner, K., Disanza, A., Confalonieri, S., Innocenti, M. and Scita, G. (2004). Regulation of actin dynamics by WASP and WAVE family proteins. *Trends Cell. Biol.* **14**, 303-311.

Tall, E. G., Spector, I., Pentyala, S. N., Bitter, I. and Rebecchi, M. J. (2000). Dynamics of phosphatidylinositol 4,5-bisphosphate in actin-rich structures. *Curr. Biol.* **10**, 743-746.